Laser and Particle Beams (2011), *29*, 383–388.

doi:10.1017/S0263034611000462

Dynamics of nanometer-scale foil targets irradiated with relativistically intense laser pulses

R. HÖRLEIN,[1,2] S. STEINKE,[3] A. HENIG,[1,2] S.G. RYKOVANOV,[1,2] M. SCHNÜRER,[3] T. SOKOLLIK,[3] D. KIEFER,[1,2] D. JUNG,[2,4] X.Q. YAN,[1,5] T. TAJIMA,[2,6] J. SCHREIBER,[1,2] M. HEGELICH,[2,4] P.V. NICKLES,[3,7] M. ZEPF,[1,8] G.D. TSAKIRIS,[1] W. SANDNER,[3] AND D. HABS[1,2]

[1]Max-Planck-Institut für Quantenoptik, Garching, Germany
[2]Fakultät für Physik, Ludwig-Maximilians-Universität München, Garching, Germany
[3]Max-Born-Institut, Berlin, Germany
[4]Los Alamos National Laboratory, Los Alamos, New Mexico
[5]State Key Lab of Nuclear Physics and Technology, Peking University, Bejing, China
[6]Photomedical Research Center, JAEA, Kyoto, Japan
[7]Gwangju Institute of Science and Technology, GIST, Gwangju, Republic of Korea
[8]Department of Physics and Astronomy, Queens University Belfast, Belfast, United Kingdom

(RECEIVED 17 June 2011; ACCEPTED 20 July 2011)

Abstract

In this paper we report on an experimental study of high harmonic radiation generated in nanometer-scale foil targets irradiated under normal incidence. The experiments constitute the first unambiguous observation of odd-numbered relativistic harmonics generated by the $\mathbf{v} \times \mathbf{B}$ component of the Lorentz force verifying a long predicted property of solid target harmonics. Simultaneously the observed harmonic spectra allow in-situ extraction of the target density in an experimental scenario which is of utmost interest for applications such as ion acceleration by the radiation pressure of an ultraintense laser.

Keywords: Frequency conversion; Laser-driven acceleration; Laser-plasma interaction; Particle-in-cell method; Plasma-generated coherent radiation

INTRODUCTION

The interaction of ultra-intense laser pulses with nanometer-scale solid density foil targets has raised a lot of interest as it promises the generation of mono-energetic ion and electron bunches via novel, more efficient acceleration mechanisms such as radiation pressure acceleration (RPA) (Bin *et al.*, 2009; Esirkepov *et al.*, 2004; Henig *et al.*, 2009; Klimo *et al.*, 2008; Robinson *et al.*, 2008; Yan *et al.*, 2008). The key to efficient RPA is to suppress heating of the target electrons (Klimo *et al.*, 2008; Robinson *et al.*, 2008, Shoucri & Afeyan, 2010) and careful control of the target surface area density (Yan *et al.*, 2008). To obtain information on these quantities, a diagnostic capable of probing the dynamics of the entire laser generated plasma during the acceleration process is necessary. We show that surface high harmonic generation (SHHG), i.e., the generation of high harmonics on the sharp plasma-vacuum interface of nanometer-scale (nm) foil targets irradiated under normal incidence allows detailed studies of crucial interaction parameters such as the target deformation and plasma density when the peak of the driving pulse interacts with the target, i.e., while the particle acceleration takes place, without requiring an additional probe beam. Moreover, our results advance the understanding of the harmonic generation process itself as previous experiments have not addressed normal incidence interactions in detail.

The generation of high-harmonic radiation from solid density bulk (Baeva *et al.*, 2006, 2007; Bulanov *et al.*, 1994; Dromey *et al.*, 2007, 2009; Hörlein *et al.*, 2010; Nomura *et al.*, 2009; Quere *et al.*, 2006; Tarasevitch *et al.*, 2007; Teubner & Gibbon, 2009; Tsakiris *et al.*, 2006) as well as foil targets (George *et al.*, 2009; Teubner *et al.*, 2004; Krushelnick *et al.*, 2008) has been studied extensively in recent years as it promises extreme-ultraviolet and soft X-ray pulses of attosecond (as) duration with unprecedented intensities (Baeva *et al.*, 2007; Tsakiris *et al.*, 2006), and is a powerful probe of the ultra-fast target dynamics. Recent

Address correspondence and reprint requests to: S. Steinke, Max-Born-Institut, D-12489 Berlin, Germany. E-mail: steinke@mbi-berlin.de

experiments have shown that the harmonics generated on solid targets are indeed phase-locked and emitted as a train of as-pulses (Hörlein *et al.*, 2010; Nomura *et al.*, 2009) and have demonstrated the efficient generation of harmonics up to the keV energy range (Dromey *et al.*, 2007). Simultaneously, high harmonic generation gives detailed insight into the laser plasma dynamics in high-intensity laser solid interactions allowing the probing of, for example, the plasma density (Quere *et al.*, 2006), magnetic fields (Tatarakis *et al.*, 2002), surface dynamics (Dromey *et al.*, 2009; Tarasevitch *et al.*, 2007), and electron heating (Krushelnick *et al.*, 2008).

In this paper, we present measurements of the harmonic emission in transmission of nm-scale (sub-20 nm) high-density ($2.7\ g/cm^3$) diamond-like carbon foils irradiated with ultra-high contrast linearly polarized laser pulses at normal incidence (Fig. 1). We show that the harmonic emission, apart from being an interesting radiation source, is a versatile probe of the ultra-fast target dynamics. The experiments give insight into the three-dimensional nature of the laser-foil interaction dynamics and allow the determination of the target density at the instant when the peak of the driving pulse interacts with it. This constitutes the first measurement of critical plasma parameters in normal incidence interactions of relativistic laser pulses with nm-scale foil targets relevant, for example, for ion acceleration (Steinke *et al.*, 2010). Moreover, the experiments confirm a central theoretical prediction in SHHG at normal incidence (Baeva *et al.*, 2006; Bulanov *et al.*, 1994, Tsakiris *et al.*, 2006) that has so far lacked conclusive experimental proof. In this case, SHHG should be dominated by the $\mathbf{v} \times \mathbf{B}$ component of the Lorentz force oscillating at twice the laser frequency. Unlike in the oblique incidence case, this should result in the generation of only odd-numbered harmonics.

HIGH HARMONIC GENERATION FROM NM-SCALE FOILS

Like in the interaction with bulk targets, two distinct mechanisms capable of generating high-order harmonics in the transmission of nm-scale foils have been identified (George *et al.*, 2009). For sub- and weakly-relativistic intensities corresponding to a normalized vector potential $a_0 = sqrt\{I_L \lambda_L^2 / 1.37 \times 10^{18}\ \mathrm{Wcm}^{-2}\ \mu\mathrm{m}^2\}$ below, or on the order of unity,

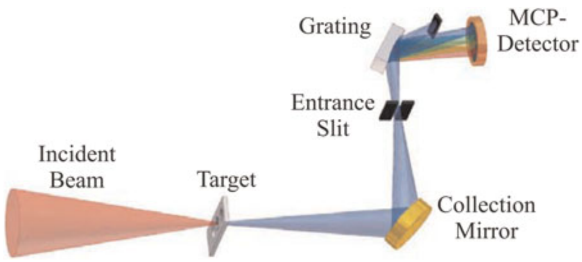

Fig. 1. (Color online) Schematic drawing of the experimental setup.

where I_L and λ_L stand for the cycle-averaged intensity and the wavelength of the incident laser light, harmonics are generated via linear mode-conversion of plasma waves (Sheng *et al.*, 2005) in the density gradient on the rear side of the foil. These plasma waves, unlike on the front side of the target, are excited indirectly by as-electron bursts propagating up the rear side density gradient. These bunches are accelerated in the electric field set up by other electron bunches generated on the front side that penetrate through the foil (George *et al.*, 2009; Teubner *et al.*, 2004). This mechanism is conventionally called coherent wake emission (CWE) (Quéré *et al.*, 2006). For larger intensities and especially in the relativistic limit ($a_0 >> 1$), harmonic radiation can also be emitted by plasma electrons close to the critical density layer coherently oscillating with velocities close to the speed of light in the driving laser field (Baeva *et al.*, 2006; Bulanov *et al.*, 1994; Tsakiris *et al.*, 2006). In the case of very thin foil targets, this mechanism can also generate harmonics emitted in the forward direction that propagate through the target, and can be observed at the rear side (George *et al.*, 2009; Krushelnick *et al.*, 2008). The predominant mechanism in a specific experiment can be determined by the characteristics of the detected harmonic spectrum. While relativistic harmonics exhibit an intensity dependent spectral cut-off, CWE harmonics do not. Instead, they have a distinct high energy cut-off determined by the maximum plasma frequency, and thus peak density in the target. In this case, the highest generated harmonic order is $q_{co} = \omega_{p,\max}/\omega_L$ where ω_L and $\omega_{p,\max} = sqrt\{n_{e,\max}\ e^2/\epsilon_0\ m_e\}$ with $n_{e,\max}$ the peak electron density are the laser and peak plasma frequency, respectively. In addition, the generation of CWE harmonics requires oblique incidence as the conditions for mode conversion cannot be fulfilled otherwise (Sheng *et al.*, 2005). In contrast, relativistic harmonics can also be generated under normal incidence in which case the electron oscillations are driven by the $\mathbf{v} \times \mathbf{B}$ component of the driving force oscillating at twice the laser frequency resulting in the generation of only odd harmonics (Tsakiris *et al.*, 2006).

In the case of a mildly relativistic laser pulse incident normally onto a thin foil the harmonic spectrum may show signatures of both harmonic generation mechanisms, which one dominates, will depend on the detailed dynamics of the interaction. Especially denting of the target in the focus will alter the interaction significantly as this result in effectively oblique incidence on the sides of the focal spot. Due to the lower intensity level in these regions of the focus, the harmonic generation will likely be dominated by CWE in such regions resulting in a spectrum containing all harmonics with a density dependent cut-off. If relativistic harmonics are also generated they will originate predominantly from the center of the focus where the intensity is highest and likely display only odd orders owing to the true normal incidence in this region. The relative efficiency of the two mechanisms will vary depending on how planar the laser target interaction is, resulting in different intensity ratios between odd and even harmonics. In addition target non-uniformities across the focal region can also influence the effective angle of incidence of the driving electric field.

SIMULATIONS

To verify this argumentation, we have conducted two-dimensional particle-in-cell (PIC) simulations of the laser foil interaction at normal incidence using the code PICWIG (Hörlein *et al.*, 2009; Rykovanov *et al.*, 2008). As will be discussed later even for the ultra-clean laser pulses employed in this experiment, the target will have expanded in the rising edge of the 45 fs pulse with $a_0 = 3.6$. Taking this into account, the simulations were initialized using a triangular density profile with a peak density of $n_0 = 100n_c$ and a linear ramp of length 25 nm on both the front and the rear side. Considering that the original target density in the experiment is approximately $480n_c$ this corresponds to a solid density foil of approximately 5 nm in original thickness. The laser pulse was Gaussian both in space and time (spot size 3 μm full width at half maximum (FWHM), duration 15 cycles FWHM in the field) and incident normally onto the target. The size of the simulation box is 6 λ_L in laser propagation direction and 15 λ_L in polarization direction. The time step is $\tau_L/400$ and the laser propagation direction spatial step correspondingly is $\lambda_L/400$ where τ_L is the period of the driving laser. The results of the simulation are depicted in Figure 2. The denting of the foil during the interaction is clearly visible in Figure 2a where the electron density near the instance when the peak of the pulse interacts with the target is shown. Figure 2b shows the harmonic spectrum emitted in the forward direction as a function of position across the target recorded at a position just behind the target surface. On-axis only odd harmonics are generated, which can only originate from relativistic electron oscillations as the condition for mode conversion necessary for CWE (Sheng *et al.*, 2005) cannot be fulfilled in this geometry while off-axis all harmonics are generated owing to the effectively oblique incidence of the driving pulse. To derive the total harmonic spectrum collected in the experiment after propagation to the detector, we sum over the spectra emitted at the different positions in the focus. The resulting power spectrum is shown in Figure 2c. The integrated spectrum contains all harmonic orders but an enhancement of odd harmonics originating from the center of the generation region is visible constituting a clear signature of relativistic harmonic generation on axis.

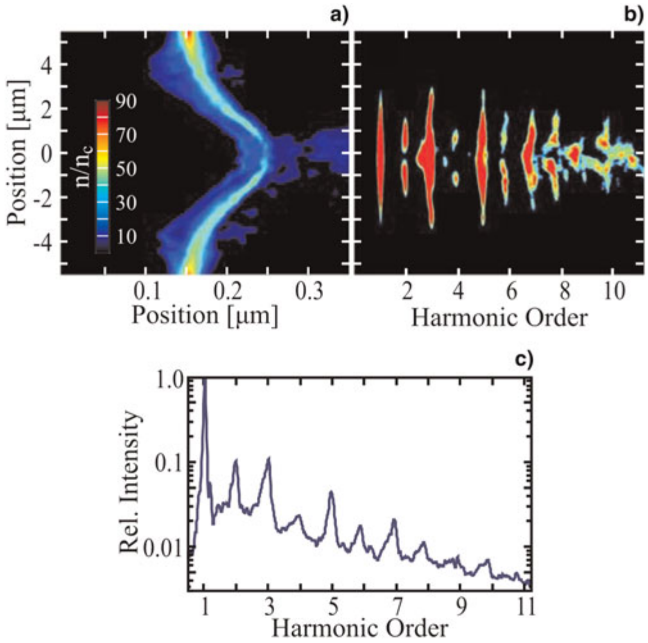

Fig. 2. (Color online) Results of two-dimensional PIC-simulations of the interaction of a relativistic laser pulse with a triangular shaped target with 25 nm gradients on each side and a peak density of $100n_c$. (**a**) show the electron density distribution at the instance when the peak of the driving pulse arrives at the initial target position (note the different length scales used to emphasize the denting of the target) and (**b**) the time integrated harmonic spectra emitted in the forward direction as a function of radial position recorded at a position just behind the target surface. A clear difference in the emission characteristics on- and off-axis is visible. Radially integrating the individual spectra in (b) to account for the collection of the signal with a mirror yields the spectrum shown in (**c**) exhibiting all harmonics with an enhancement of the odd orders.

EXPERIMENTAL RESULTS

The experiments presented in this article were conducted using the 30 TW laser facility at the Max-Born-Institute in Berlin. The Ti:sapphire laser system delivered pulses with an energy of 0.7 J and a pulse duration of 45 fs at a central wavelength of 810 nm to the target. To enhance the temporal contrast of the laser a recollimating double plasma mirror (Andreev *et al.*, 2009) was introduced into the system enhancing the temporal contrast to better than $1{:}10^{10}$ on the few picosecond scale. The beam was focused to a near diffraction-limited focal spot of 3.6 μm FWHM diameter using a dielectrically coated $f/2.5$ off-axis parabola resulting in a peak focused intensity of $I_{0,\text{peak}} = 5 \times 10^{19}$ W/cm^2 corresponding to a normalized vector potential of $a_{0,\text{peak}} \sim 5$.

Free-standing diamond-like carbon foils like the ones used in Henig *et al.* (2009) and Steinke *et al.* (2010) ranging from approximately 5 to 17 nm in thickness were irradiated under normal incidence in the focus of the driving laser beam. The radiation emitted in the laser propagation direction was collected using a spherical mirror with an unprotected gold coating positioned under an angle of 45° (see Fig. 1). The resulting line focus was placed on the entrance slit of a normal incidence ACTON VM-502 VUV-spectrometer equipped with a micro-channel-plate detector and a fiber-coupled charge-coupled device-camera. The spectrometer allowed the detection of radiation from 140 down to 50 nm corresponding to harmonics 7 to 16 of the fundamental laser wavelength.

Two typical normalized harmonic spectra obtained from targets of different thicknesses are depicted in Figure 3.

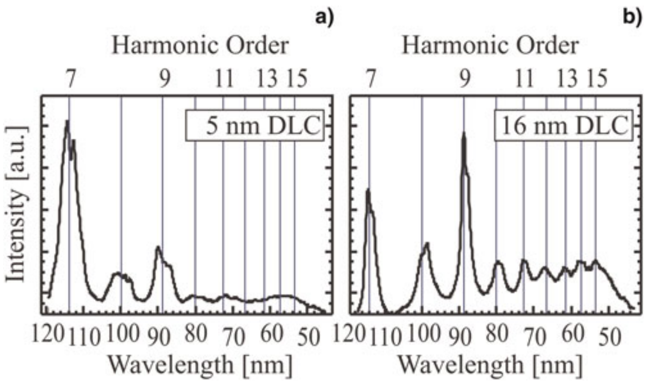

Fig. 3. (Color online) Normalized high harmonic spectra obtained from targets with two different thicknesses.

The absolute peak intensity in Figure 3a is approximately twice as big as in Figure 3b. Both spectra show odd and even harmonics with a pronounced enhancement of the odd harmonics, especially the orders of 7 (H7) and 9 (H9). The spectra do however differ significantly in the highest harmonic visible. The spectrum from the thinner target (Fig. 3a) shows harmonics up to H9 whereas radiation with significantly shorter wavelength up to H15 is generated from the thicker target (Fig. 3b).

These spectral properties suggest that the harmonics in our experiment are indeed generated by two different mechanisms as predicted by simulations, one generating predominantly odd and one producing all harmonics. The thickness dependent cut-off with higher harmonics from thicker foils in combination with the moderate intensities on the sides of the focus suggests that this part of the spectrum is generated by CWE (George *et al.*, 2009). This means that the target has to be dented significantly to facilitate motion of the plasma electrons in and out of the surface in the electric field as predicted by the simulation. The trend of higher harmonics from thicker targets is visible for all measured targets and is displayed in Figure 4, where the cut-off harmonic order and corresponding peak target density is plotted versus the original foil thickness. The peak density in the interaction region as inferred from the harmonic generation

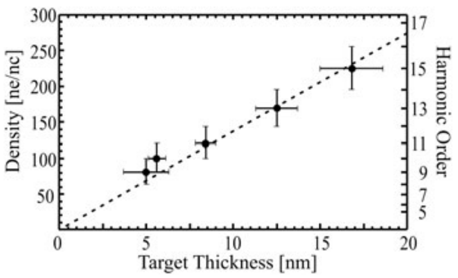

Fig. 4. Peak target density and cutoff harmonic plotted as a function of original target thickness. The dashed line corresponds to the peak density expected for a one dimensional foil expansion with a scale length of 18 nm on each side. The spectra shown in Figures 3a and 3b correspond (from left to right) to the second and the fifth data point respectively.

emitted during the most intense phase of the laser foil interaction is found to increase linearly with initial target thickness. This suggests that the target plasma expands with similar velocities in all cases resulting in densities during the interaction that are significantly lower than those of the original foil. For all studied targets, the decrease in density is consistent with an exponential density ramp with a scale length of approximately 18 nm on each side of the foil at the onset of the relativistic interaction. The dashed line in Figure 4 shows the peak target densities expected in such a scenario and is in very good agreement with the measured data. To check these values for consistency, we estimate the expansion of the foil after ionization, and prior to the relativistic interaction considering a Gaussian pulse shape on the rising edge of the 45 fs pulse. Assuming uniform energy deposition in the foil (Price *et al.*, 1995) the ion sound velocity rapidly increases over a time window of 70 fs to approximately $c_{s,\mathrm{peak}} = 5 \times 10^7\ \mathrm{cm/s}$ corresponding to a hot electron temperature $T_e \sim 5$ keV at which the plasma becomes non-collisional under our experimental conditions (Blanc *et al.*, 1996; Gibbon, 2005; Kruer, 1988). During this time, the average sound velocity is found to be $c_{s,av} \sim 2.2 \times 10^7\ \mathrm{cm/s}$ which results in an expansion by 15.4 nm in good agreement with the measured data. Thus, in addition to the determination of the target density, the experiment gives information about the target heating prior to the relativistic interaction and demonstrates a fundamental limitation of the nm-foil density at the instance of the interaction with the peak of the laser pulse which can be crucial when even thinner targets are employed.

CONCLUSIONS

In conclusion, we have presented the first experiment demonstrating the generation of high order harmonics in the transmission of few-nm-scale foil targets irradiated at normal incidence. The measurements in combination with two-dimensional PIC-simulations demonstrate that the harmonics are generated via two different mechanisms in different regions of the laser focus giving detailed insight into the dynamics of the foil target under experimental conditions also of interest, for example, for particle acceleration experiments. While non-uniformities such as denting of the target lead to effectively oblique incidence of the driving field on the sides of the focus and the generation of all harmonics in this region, only odd harmonics are generated exactly on the laser axis. This constitutes the first unambiguous demonstration of relativistic harmonic generation at normal incidence as predicted in many theoretical publications. Harmonics are mainly generated via CWE in regions of oblique incidence, which allows the determination of the instantaneous target density of the foil in the relativistic interaction. The densities inferred from the observed harmonic spectra are in good agreement with the one-dimensional expansion of the foil targets. This expansion occurs even for perfect Gaussian laser pulses and thus imposes a fundamental limit on the peak density of few-nm-scale foil targets during the relativistic part of the laser solid interaction. The experiments demonstrate that, beyond the fundamental study of the harmonic generation process itself, this method is a powerful diagnostic of the laser plasma interaction that can be employed in many experimental scenarios pertaining to efficient laser particle acceleration including RPA with circular polarization. In fact, the method does not even require any modifications to existing particle acceleration experiments except for the implementation of a pickoff optic as all the information is generated by the driving laser beam itself.

ACKNOWLEDGMENTS

We would like to thank the Berlin laser staff for their support. This work was funded in part by the DFG through SFB Transregio18 and the Cluster of Excellence Munich Center for Advanced Photonics (MAP) and by the Association EURATOM – Max-Planck-Institut für Plasmaphysik. A. H., S. G. R., D. K. and D. J. acknowledge financial support from IMPRS-APS. X. Q. Y. acknowledges financial support from the Humboldt Foundation and NSFC (10935002).

REFERENCES

ANDREEV, A.A., STEINKE, S., SOKOLLIK, T., SCHNÜRER, M., TER AVETSIYAN, S., PLATONOV, K.Y. & NICKLES, P.V. (2009). Optimal ion acceleration from ultrathin foils irradiated by a profiled laser pulse of relativistic intensity. *Phys. Plasmas* **16**, 013103.

BAEVA, T., GORDIENKO, S. & PUKHOV, A. (2006). Theory of high-order harmonic generation in relativistic laser interaction with overdense plasma. *Phys. Rev. E* **74**, 046404.

BAEVA, T., GORDIENKO, S. & PUKHOV, A. (2007). Relativistic plasma control for single attosecond pulse generation: Theory, simulations, and structure of the pulse. *Laser Part. Beams* **25**, 339–346.

BIN, J.H., LEI, A.L., YANG, X.Q., HUANG, L.G., YU, M.Y., YU, W. & TANAKA, K.A. (2009). Quasi-monoenergetic proton beam generation from a double-layer solid target using an intense circularly polarized laser. *Laser Part. Beams* **27**, 485–490.

BLANC, P., AUDEBERT, P., FALLIÈS, F., GEINDRE, J.P., GAUTHIER, J.C., SANTOS, A.D., MYSYROWICZ, A. & ANTONETTI, A. (1996). Phase dynamics of reflected probe pulses from sub-100-fs laser-produced plasmas. *J. Opt. Soc. Am. B* **13**, 118–124.

BULANOV, S.V., NAUMOVA, N.M. & PEGORARO, F. (1994). Interaction of an ultrashort, relativistically strong laser pulse with an overdense plasma. *Phys. Plasmas* **1**, 745–757.

DROMEY, B., ADAMS, D., HÖRLEIN, R., NOMURA, Y., RYKOVANOV, S.G., CARROLL, D.C., FOSTER, P.S., KAR, S., MARKEY, K., MCKENNA, P., NEELY, D., GEISSLER, M., TSAKIRIS, G.D., & ZEPF, M. (2009). Diffraction-limited performance and focusing of high harmonics from relativistic plasmas. *Nat Phys* **5**, 146–152.

DROMEY, B., KAR, S., BELLEI, C., CARROLL, D.C., CLARKE, R.J., GREEN, J.S., KNEIP, S., MARKEY, K., NAGEL, S.R., SIMPSON, P.T., WILLINGALE, L., MCKENNA, P., NEELY, D., NAJMUDIN, Z., KRUSHELNICK, K., NORREYS, P.A. & ZEPF, M. (2007). Bright multi-keV harmonic generation from relativistically oscillating plasma surfaces. *Phys. Rev. Lett.* **99**, 085001.

ESIRKEPOV, T., BORGHESI, M., BULANOV, S.V., MOUROU, G. & TAJIMA, T. (2004). Highly efficient relativistic-ion generation in the laser-piston regime. *Phys. Rev. Lett*. **92**, 175003.

GEORGE, H., QUÉRÉ, F., THAURY, C., BONNAUD, G. & MARTIN, P. (2009). Mechanisms of forward laser harmonic emission from thin overdense plasmas. *New J. Phys*. **11**, 113028.

GIBBON, P. (2005) *Short Pulse Laser Interactions with Matter*. London: Imperial College Press.

HENIG, A., STEINKE, S., SCHNÜRER, M., SOKOLLIK, T., HOERLEIN, R., KIEFER, D., JUNG, D., SCHREIBER, J., HEGELICH, B.M., YAN, X.Q., MEYER-TER-VEHN, J., TAJIMA, T., NICKLES, P.V., SANDNER, W. & HABS, D. (2009). Radiation-pressure acceleration of ion beams driven by circularly polarized laser pulses. *Phys. Rev. Lett*. **103**, 245003.

HÖRLEIN, R., RYKOVANOV, S., DROMEY, B., NOMURA, Y., TZALLAS, P., ADAMS, D., GEISSLER, M., ZEPF, M., KRAUSZ, F. & TSAKIRIS, G.D. (2009). Controlling the divergence of high harmonics from solid targets: A route toward coherent harmonic focusing. *Eur. Phys. J. D* **55**, 475–481.

HÖRLEIN, R., NOMURA, Y., TZALLAS, P., RYKOVANOV, S.G., DROMEY, B., OSTERHOFF, J., MAJOR, Z., KARSCH, S., VEISZ, L., ZEPF, M., CHARALAMBIDIS, D., KRAUSZ, F. & TSAKIRIS, G.D. (2010). Temporal characterization of attosecond pulses emitted from solid-density plasmas. *New J. Phys*. **12**.

KLIMO, O., PSIKAL, J., LIMPOUCH, J. & TIKHONCHUK, V.T. (2008). Monoenergetic ion beams from ultrathin foils irradiated by ultrahigh-contrast circularly polarized laser pulses. *Phys. Rev. ST Accel. Beams* **11**, 031301.

KRUER, W.L. (1988). The Physics of Laser Plasma Interactions. Redwood City: Addison-Wesley.

KRUSHELNICK, K., ROZMUS, W., WAGNER, U., BEG, F.N., BOCHKAREV, S.G., CLARK, E.L., DANGOR, A.E., EVANS, R.G., GOPAL, A., HABARA, H., MANGLES, S.P.D., NORREYS, P.A., ROBINSON, A.P.L., TATARAKIS, M., WEI, M.S. & ZEPF, M. (2008). Effect of relativistic plasma on extreme-ultraviolet harmonic emission from intense laser-matter interactions. *Phys. Rev. Lett.* **100**, 125005.

NOMURA, Y., HÖRLEIN, R., TZALLAS, P., DROMEY, B., RYKOVANOV, S., MAJOR, Z., OSTERHOFF, J., KARSCH, S., VEISZ, L., ZEPF, M., CHARALAMBIDIS, D., KRAUSZ, F. & TSAKIRIS, G.D. (2009). Attosecond phase locking of harmonics emitted from laser-produced plasmas. *Nat. Phys.* **5**, 124–128.

PRICE, D.F., MORE, R.M., WALLING, R.S., GUETHLEIN, G., SHEPHERD, R.L., STEWART, R.E. & WHITE, W.E. (1995). Absorption of ultrashort laser pulses by solid targets heated rapidly to temperatures 1–1000 eV. *Phys. Rev. Lett.* **75**, 252.

QUÉRÉ, F., THAURY, C., MONOT, P., DOBOSZ, S., MARTIN, P., GEINDRE, J.P. & AUDEBERT, P. (2006). Coherent Wake Emission of High-Order Harmonics from Overdense Plasmas. *Phys. Rev. Lett.* **96**, 125004.

ROBINSON, A.P.L., ZEPF, M., KAR, S., EVANS, R.G. & BELLEI, C. (2008). Radiation pressure acceleration of thin foils with circularly polarized laser pulses. *New J. Phys.* **10**, 013021.

RYKOVANOV, S.G., GEISSLER, M., MEYER-TER-VEHN, J. & TSAKIRIS, G.D. (2008). Intense single attosecond pulses from surface harmonics using the polarization gating technique. *New J. Phys.* **10**, 025025.

SHENG, Z.M., MIMA, K., ZHANG, J. & SANUKI, H. (2005). Emission of electromagnetic pulses from laser wakefields through linear mode conversion. *Phys. Rev. Lett.* **94**, 095003.

Shoucri, M. & Afeyan, B. (2010). Studies of the interaction of an intense laser beam normally incident on an overdense plasma. *Laser Part. Beams* **28**, 129–147.

Steinke, S., Henig, A., Schnürer, M., Sokollik, T., Nickles, P.V., Jung, D., Kiefer, D., Hörlein, R., Schreiber, J., Tajima, T., Yan, X.Q., Hegelich, M., Meyer-Ter-Vehn, J., Sandner, W. & Habs, D. (2010). Efficient ion acceleration by collective laser-driven electron dynamics with ultra-thin foil targets. *Laser Part. Beams* **28**, 215–221.

Tarasevitch, A., Lobov, K., Wünsche, C. & Von Der Linde, D. (2007). Transition to the relativistic regime in high order harmonic generation. *Phys. Rev. Lett.* **98**, 103902.

Tatarakis, M., Watts, I., Beg, F.N., Clark, E.L., Dangor, A.E., Gopal, A., Haines, M.G., Norreys, P.A., Wagner, U., Wei, M.S., Zepf, M. & Krushelnick, K. (2002). Laser technology: Measuring huge magnetic fields. *Nature* **415**, 280–280.

Teubner, U., Eidmann, K., Wagner, U., Andiel, U., Pisani, F., Tsakiris, G.D., Witte, K., Meyer-Ter-Vehn, J., Schlegel, T. & Foerster, E. (2004). Harmonic emission from the rear side of thin overdense foils irradiated with intense ultrashort laser pulses. *Phys. Rev. Lett.* **92**, 185001.

Teubner, U. & Gibbon, P. (2009). High-order harmonics from laser-irradiated plasma surfaces. *Rev. Mod. Phys.* **81**, 445.

Tsakiris, G.D., Eidmann, K., Meyer-Ter-Vehn, J. & Krausz, F. (2006). Route to intense single attosecond pulses. *New J. Phys.* **8**, 19.

Yan, X.Q., Lin, C., Sheng, Z.M., Guo, Z.Y., Liu, B.C., Lu, Y.R., Fang, J. X. & Chen, J.E. (2008). Generating High-Current Monoenergetic Proton Beams by a Circularly Polarized Laser Pulse in the Phase-Stable Acceleration Regime. *Phys. Rev. Lett.* **100**, 135003.